

## Synthesis of Glycerol Carbonate by Transesterification of Glycerol and Dimethyl Carbonate over KF/ $\gamma$ -Al<sub>2</sub>O<sub>3</sub> Catalyst

Zhenmin Liu,<sup>a,b,c</sup> Junwei Wang,<sup>\*a</sup> Maoqing Kang,<sup>a</sup> Ning Yin,<sup>a</sup> Xinkui Wang,<sup>a</sup>  
Yisheng Tan<sup>b</sup> and Yulei Zhu<sup>b</sup>

<sup>a</sup>Laboratory of Applied Catalysis and Green Chemical Engineering and

<sup>b</sup>State Key Laboratory of Coal Conversion, Institute of Coal Chemistry,  
Chinese Academy of Sciences, 030001 Taiyuan, P. R. China

<sup>c</sup>University of Chinese Academy of Sciences, 100049 Beijing, P. R. China

Uma série de catalisadores sólidos básicos de KF/ $\gamma$ -Al<sub>2</sub>O<sub>3</sub> foi preparada pelo método de impregnação úmida e aplicada à síntese de carbonato de glicerina (GC) a partir de glicerol e carbonato de dimetila. As influências do teor de KF e da temperatura de calcinação do catalisador na síntese foram investigadas. Os resultados mostraram que os catalisadores de KF/ $\gamma$ -Al<sub>2</sub>O<sub>3</sub> conseguem promover uma conversão eficiente de glicerol em GC. A estrutura e as propriedades dos catalisadores foram estudadas por difratometria de raios X (XRD), espectroscopia no infravermelho por transformada de Fourier (FTIR), adsorção de N<sub>2</sub>, dessorção térmica programada (TPD) de CO<sub>2</sub>, espectroscopia fotoeletrônica por raios X (XPS) e pelo método dos indicadores de Hammett. Observou-se que os catalisadores possuem vários tipos de centros básicos, como KF, KAlO<sub>2</sub>, KOH e possivelmente o íon F<sup>-</sup> coordenativamente insaturado. Os centros fortemente básicos não somente poderiam acelerar a conversão do glicerol, como também aumentar a formação do glicidol a partir da decomposição de GC. A reutilização de KF/ $\gamma$ -Al<sub>2</sub>O<sub>3</sub> mostrou que a decomposição do catalisador, que é causada principalmente pela lixiviação parcial das espécies ativas de potássio, aumenta com o número de usos. Temperaturas altas de calcinação favorecem a transformação de KF em KAlO<sub>2</sub> e amenizam a desativação do catalisador. Com base na distribuição dos produtos e nos resultados obtidos, foi proposto um mecanismo possível para a reação do glicerol com carbonato de dimetila.

A series of KF/ $\gamma$ -Al<sub>2</sub>O<sub>3</sub> solid base catalysts were prepared by a wet impregnation method and applied to the synthesis of glycerol carbonate (GC) from glycerol and dimethyl carbonate. The influences of KF loading and calcination temperature of catalyst on the synthesis were investigated. The results showed that KF/ $\gamma$ -Al<sub>2</sub>O<sub>3</sub> catalysts could promote glycerol conversion to GC efficiently. The structure and properties of the catalysts were studied by means of X-ray diffraction (XRD), Fourier transform infrared spectroscopy (FT-IR), N<sub>2</sub>-adsorption, CO<sub>2</sub>-temperature programmed desorption (TPD), X-ray photoelectron spectroscopy (XPS) and Hammett indicator method. It was found that several types of basic centers such as KF, KAlO<sub>2</sub>, KOH and possibly coordinately unsaturated F<sup>-</sup> ion existed on the catalysts. The strong basic centers could not only accelerate the conversion of glycerol, but also enhance the formation of glycidol from the decomposition of GC. The recycling of KF/ $\gamma$ -Al<sub>2</sub>O<sub>3</sub> revealed that deactivation of catalyst was strengthened with the reuse times, which was mainly caused by the partial leaching of active potassium species. High calcination temperature favored the transformation of KF to KAlO<sub>2</sub> and alleviated the deactivation of the catalyst. Based on the product distribution and obtained results, a possible reaction mechanism on reaction of glycerol with dimethyl carbonate was proposed.

**Keywords:** glycerol, dimethyl carbonate, glycerol carbonate, KF/ $\gamma$ -Al<sub>2</sub>O<sub>3</sub>

## Introduction

Biodiesel has attracted considerable attention as an alternative to the fossil fuel resources. European Union and U.S. government have promulgated mandatory regulations for the use of biodiesel in transportation fuel and on-road diesel.<sup>1</sup> However, production of biodiesel by plant oil methanolysis generates large amount of glycerol (about 10 wt.%) as an unavoidable by-product, which has to be valorized to improve the economic competitiveness of biodiesel.<sup>2</sup> Therefore, transformation of glycerol into value-added products is of great significance. So far, several routes for glycerol conversion have been reported, such as selective oxidation, reduction, etherification, esterification, polymerization, transesterification, etc.<sup>3,4</sup>

Among the various downstream products of glycerol, glycerol carbonate (4-hydroxymethyl-2-oxo-1,3-dioxolane, GC) represents an important and potential glycerol derivative that shows low toxicity and volatility, biodegradability, high boiling point, etc.<sup>5</sup> GC has been widely used as a solvent in the cosmetics industry, as a membrane component for gas separation, as a component of coatings and detergents, as a precursor of glycidol, and as a monomer in preparing polycarbonate and polyurethane.<sup>6-8</sup>

GC can be synthesized from glycerol and different reagents including CO, CO<sub>2</sub>, phosgene, urea and organic carbonates. Among these raw materials, CO or phosgene is practically limited due to their toxicity and safety issues at both laboratory and industrial scales.<sup>9-11</sup> The direct carbonation of glycerol with CO<sub>2</sub> is thermodynamically limited and only gives very low yield even under harsh reaction conditions.<sup>12,13</sup> The disadvantages of preparing GC from glycerol and urea lead to the creation of large amounts of ammonia and the difficulty in separating the undesired by-products like isocyanic acid and biuret.<sup>14,15</sup> Although GC may be obtained from glycerol and ethylene carbonate by transesterification, ethylene glycol is produced as by-product which makes the separation of products difficult because of their high boiling points.<sup>16</sup> Compared with these ways, transesterification of glycerol with dimethyl carbonate (DMC) for GC preparation is considered as the promising approach for industrial application due to the mild reaction conditions, easy separation, simple process and high GC yield.<sup>17-19</sup>

Several catalysts have been employed to promote this reaction efficiently. Kim *et al.*<sup>20</sup> prepared GC in the presence of a lipase catalyst Novozym 435. However, the process is plagued by long reaction time, inconvenient removal of THF solvent and the sensitivity of lipase to environment. Recently, some homogeneous catalysts

have been reported, they are tetra-*N*-butylammonium bromide, K<sub>2</sub>CO<sub>3</sub>, NaOH, etc.<sup>8,16,21,22</sup> In spite of the high catalytic activity, these catalysts are less preferable in view of difficulty in separation of the spent catalyst from the reaction mixture and their poor reusability. To meet the requirement of future commercial production, development of efficient heterogeneous and recyclable catalyst is thus highly desirable. Ochoa-Gómez *et al.*<sup>16</sup> found that the basic catalysts were more active than the acidic ones, and their catalytic activity depended on the basic strength and basicity of catalysts. Among the evaluated catalysts, CaO was found to be the best basic catalyst and gave 95% of GC yield. However, CaO was easily deactivated after adsorbing trace amount of water or CO<sub>2</sub>. Alvarez *et al.*<sup>18</sup> prepared a series of Mg/Al mixed oxides from hydrotalcite and applied to the synthesis of GC as a solid base catalyst. 97% of glycerol conversion and 93% of GC yield were obtained under the optimized conditions. Takagaki *et al.*<sup>23</sup> stated that the uncalcined hydrotalcite with hydromagnesite phase could also promote GC formation.

A number of reports have shown that the basic catalysts can accelerate the transesterification reaction efficiently. Besides CaO and hydrotalcite-like catalysts, alumina loaded KF also possesses strong basic sites, which can be prepared by simple impregnation and has been applied to various base-catalyzed reactions such as elimination, addition, condensation, epoxidation, transesterification, etc.<sup>24-26</sup> So far, there are few reports concerning the application of KF/ $\gamma$ -Al<sub>2</sub>O<sub>3</sub> as a solid base catalyst for the synthesis of GC from glycerol and DMC. Moreover, few reports discussed the effect of basic strength on the activity and selectivity of the catalyst in this process.

In this work, a series of KF/ $\gamma$ -Al<sub>2</sub>O<sub>3</sub> catalysts were prepared by an impregnation method and used to the synthesis of GC from glycerol and DMC. The catalytic activities, surface properties and the reusability of catalysts were studied.

## Experimental

### Materials

Glycerol, KF and biphenyl were purchased from Tianjin Tianli Chemical Reagent Co., Ltd. DMC was obtained from Tangshan Chaoyang Chemical Engineering Co., Ltd. Glycidol (95%) and GC (90%) for gas chromatography analysis were purchased from Tianjin Kermel Chemical Reagent Co., Ltd. and TCI (Shanghai) Development Co. Ltd., respectively. DMC was distilled before use. All other reagents were used directly as received.

### Catalyst preparation

The KF/ $\gamma$ -Al<sub>2</sub>O<sub>3</sub> catalysts were prepared by a wet impregnation method. In a typical process, 0.4266 g, 0.9005 g, 1.4301 g, 3.4730 g and 6.6301 g of KF·2H<sub>2</sub>O were separately dissolved in 7.5 mL of distilled water to obtain several KF solutions. 5 g of  $\gamma$ -Al<sub>2</sub>O<sub>3</sub> was added into the above KF solutions, respectively. The mixture was stirred at room temperature for 10 min and dried at 110 °C for 12 h. The obtained samples were calcined at 100-800 °C for 5 h. Finally, the solids were crushed into particles for use as catalyst.

### Catalyst characterization

X-ray diffraction (XRD) was measured on a Siemens D8 advance powder X-ray diffractometer using Ni-filtered Cu K $\alpha$  radiation over a 2 $\theta$  range of 5-80° with a step size of 0.02° at a scanning speed of 2° min<sup>-1</sup>.

Fourier transform infrared spectroscopy (FT-IR) data were collected on a Nicolet 380 FTIR instrument over the scanning range of 400-4000 cm<sup>-1</sup> at a resolution of 4.0 cm<sup>-1</sup>. The catalyst sample was diluted with KBr at the ratio of 1:200 and pressed into a disk.

The surface basic properties of the catalysts were measured by CO<sub>2</sub> temperature programmed desorption (TPD) using a TPD flow system equipped with a TCD detector (CHEMBET-3000 TPR/TPD, Quantachrome Instruments, USA). Experiments were carried out in the temperature range of 40-500 °C. Before TPD experiments, the samples (about 100 mg) were pretreated at 350 °C in a flow of nitrogen (20 mL min<sup>-1</sup>). The particle size of the catalyst was in the range of 40-60 mesh.

The basic strength and basicity of the solid catalysts were determined by the Hammett indicator. About 100 mg of the catalyst was ultrasonicated in 5 mL cyclohexane containing Hammett indicator and then the catalyst was left still for one hour to achieve equilibration. The basicity (expressed in mmol g<sup>-1</sup>) of the catalysts was measured using Hammett indicator–benzene carboxylic acid (0.05 mol L<sup>-1</sup> anhydrous cyclohexane solution) titration. In typical experiment, the following Hammett indicators were used: bromothymol blue (H<sub>+</sub>=7.2), phenolphthalein (H<sub>+</sub>=9.8), 2,4-dinitroaniline (H<sub>+</sub>=15.0) and 4-nitroaniline (H<sub>+</sub>=18.4).

The surface area and pore volume of the catalyst were measured by nitrogen adsorption at 77.3 K on a Tristar 3000 surface area and porosity analyzer (USA). High purity nitrogen (99.99%) was used in this analysis. Prior to the measurement, the catalysts were outgassed at 200 °C for 2 h under vacuum.

X-ray photoelectron spectroscopy (XPS) was used to measure the elemental composition on the catalyst surface and the data were collected on an XSAM800 spectrometer (KRATOS). Al K $\alpha$  radiation ( $h\nu = 1486.6$  eV) was used as the X-ray source.

### Catalytic reaction

For this transesterification reaction, glycerol (18.40 g, 0.2 mol), DMC (54.0 g, 0.6 mol) and the catalyst (4 wt.% of glycerol) were added into a three-neck round-bottom flask equipped with a mechanical stirring bar, a thermometer and a condenser connected to a liquid dividing head for separating the formed methanol. The mixture was heated to 80 °C and kept for 1.5 h under stirring. After reaction, the mixture was filtered to remove the catalyst. The liquid solution was distilled at 50 °C under reduced pressure to remove methanol and DMC.

### Procedure for recycling the catalyst

After reaction, the filtered catalysts were washed twice with 100 mL methanol, dried at 110 °C for 2 h and then collected for the next run.

### Product analysis

The product was analyzed on a gas chromatograph (GC-2014 Shimadzu, Japan) with a CBP-20 capillary column (25 m × 0.25 mm × 0.25  $\mu$ m) and a flame ionization detector. The capillary column temperature was started at 75 °C and maintained for 5 min, then raised at a rate of 30 °C min<sup>-1</sup> up to 240 °C and maintained for 30 min. The detector and injection temperature were kept at 280 °C and 250 °C, respectively. Nitrogen was used as the carrier gas. Biphenyl was chosen as the internal standard for the quantitative analysis of products.

## Results and Discussion

### Catalyst characterization

For the KF/ $\gamma$ -Al<sub>2</sub>O<sub>3</sub> catalyst, solid state reactions between KF and  $\gamma$ -Al<sub>2</sub>O<sub>3</sub> occurred during the calcination process and several new phases such as K<sub>3</sub>AlF<sub>6</sub>, KOH, KAlO<sub>2</sub> and [Al–OH···F<sup>-</sup>] might be formed.<sup>25</sup> The new phases might constitute the strong basic centers and provided the catalytic activity for the transesterification. To find out the actual active phases, XRD was used to learn the structure of KF/ $\gamma$ -Al<sub>2</sub>O<sub>3</sub> catalysts with various KF loading. The patterns are shown in Figure 1. The diffraction peaks of  $\gamma$ -Al<sub>2</sub>O<sub>3</sub> (Figure 1a) were in

good agreement with the International Centre for Diffraction Data powder diffraction file (PDF) 29-0063. When 5 wt.% of KF was loaded on  $\gamma$ -Al<sub>2</sub>O<sub>3</sub>, the catalyst displayed similar XRD patterns (Figure 1b) to that of  $\gamma$ -Al<sub>2</sub>O<sub>3</sub>, indicating that KF or its derivatives were highly dispersed on the surface of the support, or their amounts was smaller than those detectable via the XRD technique. When the KF loading rose up to 15 wt.%, the diffraction peaks at  $2\theta = 29.8^\circ, 36.7^\circ, 42.8^\circ, 53.2^\circ$  and  $62.3^\circ$  attributed to K<sub>3</sub>AlF<sub>6</sub> (PDF 03-0615) were observed in Figure 1c. Meanwhile, the weak peaks of KAlO<sub>2</sub> (PDF 53-0809) appeared at  $2\theta = 32.7^\circ, 35.9^\circ, 38.6^\circ, 46.9^\circ$  and  $58.5^\circ$ . The characteristic peaks of K<sub>3</sub>AlF<sub>6</sub> and KAlO<sub>2</sub> were strengthened gradually with further increasing KF loading, as illustrated in Figure 1d. In the XRD pattern (Figure 1e) of 45 wt.% KF/ $\gamma$ -Al<sub>2</sub>O<sub>3</sub>, a new diffraction peak appearing at  $2\theta = 30.9^\circ$  was ascribed to KOH, as supported by reference.<sup>27</sup>

As reported, the formation of KOH was inevitable in company with K<sub>3</sub>AlF<sub>6</sub>.<sup>28</sup> However, no peaks related to KOH were observed in XRD pattern of the 15 wt.% KF/ $\gamma$ -Al<sub>2</sub>O<sub>3</sub>, whereas peaks of KAlO<sub>2</sub> began to appear. When the KF loading increased up to 45 wt.%, the characteristic peak of KOH appeared, meanwhile, the peak intensity of  $\gamma$ -Al<sub>2</sub>O<sub>3</sub> decreased gradually, representing that the formed KOH reacted with  $\gamma$ -Al<sub>2</sub>O<sub>3</sub> and was converted to KAlO<sub>2</sub>. This also indicated that the redundant KOH was accumulated on the catalyst surface and was detected by XRD. Thus, it was inferred that KAlO<sub>2</sub> resulted from the interaction of KOH with  $\gamma$ -Al<sub>2</sub>O<sub>3</sub>. These results clearly showed that the loaded KF reacted with  $\gamma$ -Al<sub>2</sub>O<sub>3</sub> and formed various new phases.

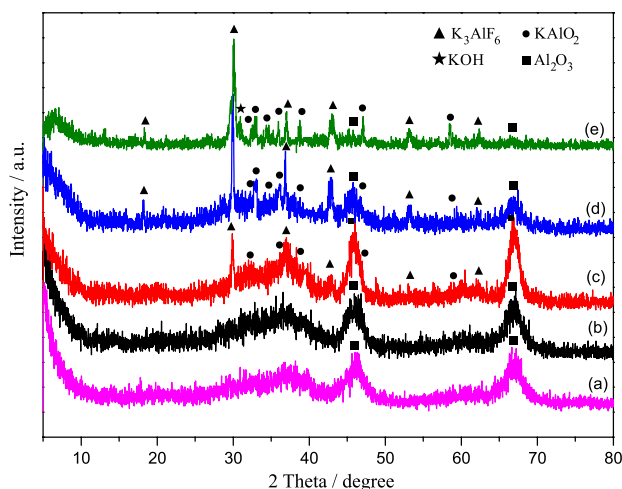


**Figure 1.** XRD patterns of  $\gamma$ -Al<sub>2</sub>O<sub>3</sub> and KF/ $\gamma$ -Al<sub>2</sub>O<sub>3</sub> with different KF loading calcined at 400 °C: (a)  $\gamma$ -Al<sub>2</sub>O<sub>3</sub>, (b) 5 wt.% KF/ $\gamma$ -Al<sub>2</sub>O<sub>3</sub>, (c) 15 wt.% KF/ $\gamma$ -Al<sub>2</sub>O<sub>3</sub>, (d) 30 wt.% KF/ $\gamma$ -Al<sub>2</sub>O<sub>3</sub>, (e) 45 wt.% KF/ $\gamma$ -Al<sub>2</sub>O<sub>3</sub>.

Additionally, the decrease of peak intensity of  $\gamma$ -Al<sub>2</sub>O<sub>3</sub> also indicated that its crystal structure was destroyed

through the solid-state reaction between KF and  $\gamma$ -Al<sub>2</sub>O<sub>3</sub>. Accordingly, the surface area and pore volume decreased and the pore size of catalyst increased with the KF loading. These data are tabulated in Table 1.

**Table 1.** The surface area and pore volume of KF/ $\gamma$ -Al<sub>2</sub>O<sub>3</sub> catalysts

Catalysts	BET area / (m <sup>2</sup> g <sup>-1</sup> )	Pore volume / (cm <sup>3</sup> g <sup>-1</sup> )	Pore size / nm
$\gamma$ -Al <sub>2</sub> O <sub>3</sub>	255	0.42	6.52
5 wt.% KF/ $\gamma$ -Al <sub>2</sub> O <sub>3</sub>	244	0.39	6.55
15 wt.% KF/ $\gamma$ -Al <sub>2</sub> O <sub>3</sub>	189	0.33	7.10
30 wt.% KF/ $\gamma$ -Al <sub>2</sub> O <sub>3</sub>	76	0.13	7.39
45 wt.% KF/ $\gamma$ -Al <sub>2</sub> O <sub>3</sub>	18	0.05	10.23

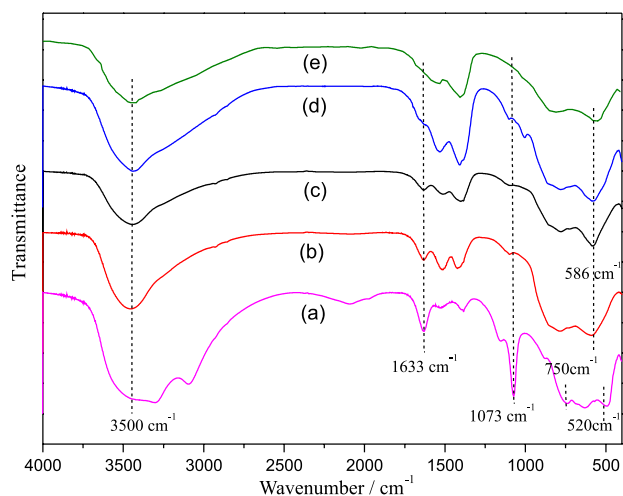


**Figure 2.** FT-IR spectra of  $\gamma$ -Al<sub>2</sub>O<sub>3</sub> and KF/ $\gamma$ -Al<sub>2</sub>O<sub>3</sub> catalysts with various KF loading: (a)  $\gamma$ -Al<sub>2</sub>O<sub>3</sub>, (b) 5 wt.% KF/ $\gamma$ -Al<sub>2</sub>O<sub>3</sub>, (c) 15 wt.% KF/ $\gamma$ -Al<sub>2</sub>O<sub>3</sub>, (d) 30 wt.% KF/ $\gamma$ -Al<sub>2</sub>O<sub>3</sub>, (e) 45 wt.% KF/ $\gamma$ -Al<sub>2</sub>O<sub>3</sub>.

Figure 2 gives the FT-IR spectra of  $\gamma$ -Al<sub>2</sub>O<sub>3</sub> and KF/ $\gamma$ -Al<sub>2</sub>O<sub>3</sub> catalysts. As shown in Figure 2a, the characteristic bands at 3500 cm<sup>-1</sup> and 1633 cm<sup>-1</sup> were attributed to the stretching vibration and bending vibration of the OH group on  $\gamma$ -Al<sub>2</sub>O<sub>3</sub>, respectively. The band at 1073 cm<sup>-1</sup> was assigned to Al–O–Al symmetric stretching vibrations. The bands appearing between 520 and 750 cm<sup>-1</sup> was related to the vibrations of Al–O bonds corresponding to aluminum ions in octahedral and tetrahedral environments.<sup>29</sup> Their band intensity decreased and even disappeared with the increasing KF loading, indicating that  $\gamma$ -Al<sub>2</sub>O<sub>3</sub> reacted with KF. At the same process, a new peak at 586 cm<sup>-1</sup> appeared which belonged to the Al–F stretching vibration in K<sub>3</sub>AlF<sub>6</sub>.<sup>26</sup> The peak at 3500 cm<sup>-1</sup> in Figure 2b-d was related to the stretching vibration of the Al–O–K group in KAlO<sub>2</sub> and became broader with increasing KF loading.<sup>30</sup> Qiu *et al.*<sup>27</sup> proved that even the pure KOH showed a weak band at 3502 cm<sup>-1</sup>. Thus, the adsorption peak at about 3500 cm<sup>-1</sup> was mainly ascribed

to  $\text{KAlO}_2$ . The FT-IR data further confirmed the formation of  $\text{K}_3\text{AlF}_6$ ,  $\text{KOH}$  and  $\text{KAlO}_2$  in the solid interaction of  $\text{KF}$  and  $\text{Al}_2\text{O}_3$ .

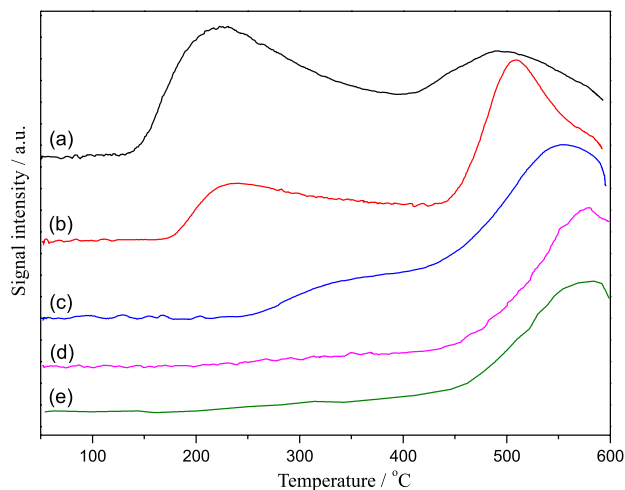


**Figure 3.**  $\text{CO}_2$ -TPD profiles of  $\text{KF}/\gamma\text{-Al}_2\text{O}_3$  with different KF loading calcined at  $400\text{ }^\circ\text{C}$ : (a) 5 wt.%  $\text{KF}/\gamma\text{-Al}_2\text{O}_3$ , (b) 10 wt.%  $\text{KF}/\gamma\text{-Al}_2\text{O}_3$ , (c) 15 wt.%  $\text{KF}/\gamma\text{-Al}_2\text{O}_3$ , (d) 30 wt.%  $\text{KF}/\gamma\text{-Al}_2\text{O}_3$ , (e) 45 wt.%  $\text{KF}/\gamma\text{-Al}_2\text{O}_3$ .

$\text{CO}_2$  temperature programmed desorption was utilized to study the basic properties of  $\text{KF}/\gamma\text{-Al}_2\text{O}_3$  catalysts. The  $\text{CO}_2$ -TPD curves of  $\text{KF}/\gamma\text{-Al}_2\text{O}_3$  catalysts with different KF loading are shown in Figure 3. Three desorption peaks appeared in  $\text{CO}_2$ -TPD curves at about 225, 340 and  $490\text{--}580\text{ }^\circ\text{C}$ . They represented the weak, medium and strong basic centers of the  $\text{KF}/\gamma\text{-Al}_2\text{O}_3$  catalyst, respectively. It was found from the desorption peak area in Figure 3a-c that the number of the strong basic centers of the  $\text{KF}/\gamma\text{-Al}_2\text{O}_3$  catalyst increased markedly with the KF loading up to 15 wt.%. This could be ascribed to the formation of much more strong basic centers which were regarded as the active centers for the transesterification reaction.<sup>31,32</sup> However, the basic sites (shown in Figure 3d-e) of  $\text{KF}/\gamma\text{-Al}_2\text{O}_3$  catalysts were reduced gradually with the further increase of KF loading. The XRD patterns had indicated that  $\text{K}_3\text{AlF}_6$  was easily formed and aggregated at high KF loading. Hence, the decrease of strong basic sites for  $\text{KF}/\gamma\text{-Al}_2\text{O}_3$  catalysts at high KF loading might be attributed to the coverage by  $\text{K}_3\text{AlF}_6$  and the structure damage resulting from the reaction between  $\text{KF}$  and  $\gamma\text{-Al}_2\text{O}_3$ .

The basic strength and basicity of the  $\text{KF}/\gamma\text{-Al}_2\text{O}_3$  catalysts were measured quantitatively using Hammett indicators. The results are shown in Table 2. The carrier  $\gamma\text{-Al}_2\text{O}_3$  was amphoteric and could not change the color of bromothymol blue ( $H_- = 7.2$ ). Its basic strength were improved by impregnating  $\text{KF}$  and accordingly the color of phenolphthalein ( $H_- = 9.8$ ) could be changed from white to red. However, all the  $\text{KF}/\gamma\text{-Al}_2\text{O}_3$  catalysts could not change

the color of 2,4-dinitroaniline ( $H_- = 15.0$ ). This indicated that the basic strength of  $\text{KF}/\gamma\text{-Al}_2\text{O}_3$  catalysts was in the range of 9.8-15.0 and the catalyst could be regarded as strong base according to Tanabe's definition.<sup>33</sup> Moreover, the basicity of  $\gamma\text{-Al}_2\text{O}_3$  was enhanced by impregnating  $\text{KF}$  and the maximum  $0.298\text{ mmol g}^{-1}$  was taken when 15 wt.%  $\text{KF}$  was loaded. Exorbitant  $\text{KF}$  loading would reduce the basicity of catalyst, probably caused by the coverage of the conglomerated  $\text{K}_3\text{AlF}_6$  and the reduction of surface area of the catalysts. The results well corresponded with the  $\text{CO}_2$ -TPD characterization and the similar phenomenon was reported in references.<sup>34,35</sup>

**Table 2.** Basic strength and basicity of  $\text{KF}/\gamma\text{-Al}_2\text{O}_3$  with various KF loading, characterized by Hammett indicators

KF loading / wt.%	Basic strength ( $H_-$ )	Basicity / ( $\text{mmol g}^{-1}$ )
0	< 7.2	–
5	9.8-15.0	0.061
10	9.8-15.0	0.176
15	9.8-15.0	0.298
30	9.8-15.0	0.216
45	9.8-15.0	0.183

#### Synthesis of GC from glycerol and DMC catalyzed by $\text{KF}/\gamma\text{-Al}_2\text{O}_3$

From Table 3, it was seen that  $\gamma\text{-Al}_2\text{O}_3$  could not promote the transformation of glycerol into GC.  $\text{KF}\cdot 2\text{H}_2\text{O}$  had unsatisfied activity for GC formation, and 48.7% of glycerol conversion was obtained after reacting at  $80\text{ }^\circ\text{C}$  for 1.5 h. However, above 99% of glycerol conversion was gained under the same reaction conditions as GC synthesis when  $\text{KF}\cdot 2\text{H}_2\text{O}$  was calcined at  $400\text{ }^\circ\text{C}$  for 3 h. Since glycerol is strongly hydrophilic, adsorbing trace amount of water from environment is unavoidable. Ando *et al.*<sup>25</sup> found that water played an important role in determining the activity of the catalyst. They believed that an active basic site involving a coordinately unsaturated  $\text{F}^-$  ion [ $\text{Al}\text{--}\text{OH}\cdots\text{F}^-$ ] was formed through the strong H-bond interaction. Zhu *et al.*<sup>36</sup> also reported that neutral  $\text{KF}$  adsorbed trace amount of water vapor and formed a similar basic site. Obviously, the high activity of  $\text{KF}$  for glycerol conversion was related to the formation of a coordinately unsaturated  $\text{F}^-$  ion through adsorbing trace amount of water. As to the lower activity of  $\text{KF}\cdot 2\text{H}_2\text{O}$ , long time was taken to lose crystal water and then produced coordinately unsaturated  $\text{F}^-$  ion. Thus, it was reasonable to obtain lower catalytic activity of  $\text{KF}\cdot 2\text{H}_2\text{O}$  than that of  $\text{KF}$ .

Table 3 shows the catalytic performance of  $\text{KF}/\gamma\text{-Al}_2\text{O}_3$  catalysts. It was found that glycerol conversion and GC

**Table 3.** The effect of different catalysts on the synthesis of glycerol carbonate

Catalyst	Conversion / %	Selectivity / %			Yield of GC / %
		GC	Glycidol	Glycerol dicarbonate	
$\gamma$ -Al <sub>2</sub> O <sub>3</sub>	0	0	0	0	0
K <sub>3</sub> AlF <sub>6</sub>	0	0	0	0	0
KF <sup>a</sup>	99.4	58.8	31.4	9.8	58.4
KF·2H <sub>2</sub> O	48.7	64.3	25.8	9.9	31.3
KOH	100	38.3	42.5	19.2	38.3
KAlO <sub>2</sub>	99.1	95.3	4.7	0	94.4
5 wt.% KF/ $\gamma$ -Al <sub>2</sub> O <sub>3</sub>	52.6	67.4	32.6	0	35.5
10 wt.% KF/ $\gamma$ -Al <sub>2</sub> O <sub>3</sub>	93.5	85.9	14.0	0.1	80.3
15 wt.% KF/ $\gamma$ -Al <sub>2</sub> O <sub>3</sub>	96.1	98.1	1.5	0.4	94.3
15 wt.% KF/ $\gamma$ -Al <sub>2</sub> O <sub>3</sub> <sup>b</sup>	96.2	97.9	1.6	0.5	94.2
15 wt.% KF/ $\gamma$ -Al <sub>2</sub> O <sub>3</sub> <sup>c</sup>	72.7	74.4	25.3	0.3	54.1
30 wt.% KF/ $\gamma$ -Al <sub>2</sub> O <sub>3</sub>	99.3	91.9	6.0	2.1	91.3
45 wt.% KF/ $\gamma$ -Al <sub>2</sub> O <sub>3</sub>	99.8	86.4	10.3	3.3	86.2

Reaction conditions: catalyst content: 4 wt.% based on the glycerol weight; n(glycerol):n(DMC) = 1:3; reaction temperature: 80 °C; reaction time: 1.5 h. Calcination conditions: 400 °C for 5 h. <sup>a</sup>KF was calcined at 400 °C for 3 h; <sup>b</sup>calcination conditions: 100 °C for 5 h; <sup>c</sup>calcination conditions: 600 °C for 5 h.

yield markedly increased by introducing KF onto  $\gamma$ -Al<sub>2</sub>O<sub>3</sub>. As described in Table 2, the basic strength of  $\gamma$ -Al<sub>2</sub>O<sub>3</sub> increased after KF loading. Accordingly, the catalytic activity was improved greatly, indicating that the high basic strength facilitated the conversion of glycerol. As KF loading was increased up to 15 wt.%, the catalytic activities and selectivity of KF/ $\gamma$ -Al<sub>2</sub>O<sub>3</sub> catalysts increased. They possessed the same basic strength and the increased basicity with KF loading increased, presenting that the basicity favored the glycerol conversion at the given basic strength.

However, further elevating KF loading only resulted in the loss of GC selectivity. In the previous XRD characterization, it had been indicated that the amount of strong basic sites such as KAlO<sub>2</sub>, KOH increased with the KF loading. In the catalytic performance, pure KOH with the basic strength above 18.4 gave a total glycerol conversion and 42.5% of selectivity to glycidol which was produced from the decomposition of GC. Therefore, it was clearly inferred that too much strong basic sites on the catalyst promoted the decomposition of GC to glycidol. Bai *et al.*<sup>19</sup> also stated that the too strong base led to the generation of glycidol.

The influence of calcination temperature on catalytic activity of KF/ $\gamma$ -Al<sub>2</sub>O<sub>3</sub> was also investigated. The results are displayed in Table 3. No obvious changes for glycerol conversion and GC selectivity were observed for 15 wt.% KF/ $\gamma$ -Al<sub>2</sub>O<sub>3</sub> catalysts calcined at 100 °C and 400 °C, respectively. Compared with those, KF/ $\gamma$ -Al<sub>2</sub>O<sub>3</sub> calcined at 600 °C showed lower activity, probably due to the transformation of active species at elevated

temperature, although their XRD patterns (shown in Figure 4a-b and Figure 1c) were similar. Thus, it was deduced that [Al–OH··F] phase might act an important role in glycerol conversion, especially at the low calcination temperature. With the calcination temperature increased, [Al–OH··F] phase was destroyed and new basic phases such as KOH, KAlO<sub>2</sub> were formed and provided new active basic sites to promote the conversion of glycerol. However, at the higher temperatures, excessive dehydroxyl, structure collapse and the formation of inactive AlF<sub>3</sub> would weaken the activity of the catalyst seriously. Accordingly, inactive AlF<sub>3</sub> (PDF 44-0231) was detected in XRD pattern (Figure 4c) of 15 wt.% KF/ $\gamma$ -Al<sub>2</sub>O<sub>3</sub> catalyst calcined at

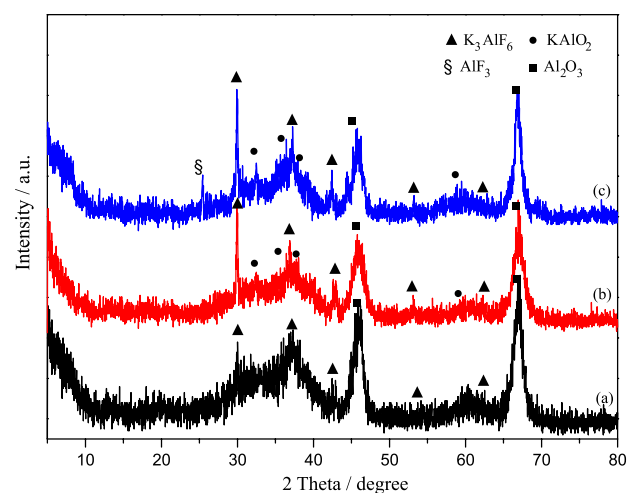


**Figure 4.** XRD patterns of 15 wt.% KF/ $\gamma$ -Al<sub>2</sub>O<sub>3</sub> catalyst calcined at different temperatures: (a) 100 °C, (b) 600 °C, (c) 800 °C.

800 °C. Ando *et al.*<sup>25</sup> and Zhu *et al.*<sup>36</sup> reported the solid state reactions occurred at various temperatures for KF/ $\gamma$ -Al<sub>2</sub>O<sub>3</sub> catalyst and the [Al–OH...F<sup>-</sup>] structure, KOH, KAlO<sub>2</sub>, K<sub>3</sub>AlF<sub>6</sub> and AlF<sub>3</sub> were found.

The characterization and catalytic performance of KF/ $\gamma$ -Al<sub>2</sub>O<sub>3</sub> have indicated that various basic sites existed on the surface of KF/ $\gamma$ -Al<sub>2</sub>O<sub>3</sub> catalyst. To learn the effect of these basic sites on reaction, pure KF,  $\gamma$ -Al<sub>2</sub>O<sub>3</sub>, K<sub>3</sub>AlF<sub>6</sub>, KAlO<sub>2</sub> and KOH were tested as catalyst, respectively. As displayed in Table 3, the pure  $\gamma$ -Al<sub>2</sub>O<sub>3</sub> and K<sub>3</sub>AlF<sub>6</sub> had no catalytic activity. In contrast, KF, KAlO<sub>2</sub> and KOH could promote the conversion of glycerol efficiently. According to our previous work and the opened literature,<sup>28,37</sup> it can be confirmed that [Al–OH...F<sup>-</sup>], KAlO<sub>2</sub> and KOH should be the main active species on KF/ $\gamma$ -Al<sub>2</sub>O<sub>3</sub> catalyst for GC synthesis.

#### Catalyst stability

The stability of a solid base catalyst is a very important factor for its industrial application. The potassium cation leaching from KF/ $\gamma$ -Al<sub>2</sub>O<sub>3</sub> catalysts has been reported in the literature.<sup>38</sup> The cation leaching in the form of homogeneous phase can lead to catalyst deactivation, product contamination and limit the catalyst reutilization in a subsequent batch process.<sup>39</sup> Thus, it is important to investigate if the K leached from KF/ $\gamma$ -Al<sub>2</sub>O<sub>3</sub> could form active homogeneous species in the solution. For that, the KF/ $\gamma$ -Al<sub>2</sub>O<sub>3</sub> catalyst was filtrated off after 1.0 h of reaction time (73% of glycerol conversion) and then the reaction was continued for 0.5 h. A conversion of 80.2% was obtained. It seemed that part of active species might leach from the catalyst and perform as homogeneous ones. However, the glycerol conversion was lower than that of reaction without removal of catalyst at the same reaction time, demonstrating that the filtrated catalyst performed catalytic activity in the form of heterogeneous phase and played more important role in glycerol conversion as compared with the leached active species. Thus, the heterogeneous phase was the main active species for glycerol conversion.

The recycling of 15% KF/ $\gamma$ -Al<sub>2</sub>O<sub>3</sub> was executed because of its high catalytic activity and GC selectivity. The operation procedure was described in sections Catalytic reaction and Procedure for recycling the catalyst. The

results are displayed in Table 4. It was shown that the glycerol conversion and GC selectivity were basically unchanged when the catalyst was reused once. The glycerol conversion decreased in the continued recycling. Generally, the deactivation of catalyst results from the coverage of active site, sintering of the active phase, poisoning of active center and the loss of active ingredient.<sup>40</sup> To find the truth of catalyst deactivation, N<sub>2</sub> adsorption, XPS characterizations were performed.

**Table 4.** The reusability of 15 wt.% KF/ $\gamma$ -Al<sub>2</sub>O<sub>3</sub> catalyst

Recycling times	Conversion / %	Selectivity for GC / %	Yield of GC / %
Fresh catalyst	96.1	98.1	94.3
1	96.1	97.0	93.2
2	96.2	95.4	91.8
3	92.5	95.2	88.1
4	90.6	94.8	85.9

Reaction conditions: catalyst content: 4 wt.% based on the glycerol weight; n(glycerol):n(DMC) = 1:3; reaction temperature: 80 °C; reaction time: 1.5 h. Calcination conditions: 400 °C for 5 h.

The surface area and pore volume of the fresh and reused catalysts are given in Table 5. The first recycling gave similar activity to that of the fresh catalyst, although it possessed a lower surface area and pore volume. The reduction of the surface area and pore volume was mainly ascribed to the blockage of the catalyst microspore by the residual products, which could not be removed entirely by washing with methanol. The sintering of active phase on the catalyst surface could be ignored because of the low reaction temperature. The XPS analysis data of the fresh and recycled catalysts are given in Table 6. It could be seen that K abundance on the catalyst surface decreased gradually with the recycling times. Moreover, the formed

**Table 5.** The surface area and pore volume of KF/ $\gamma$ -Al<sub>2</sub>O<sub>3</sub> catalyst in recycling

Recycle times	BET area / (m <sup>2</sup> g <sup>-1</sup> )	Pore volume / (cm <sup>3</sup> g <sup>-1</sup> )
Fresh catalyst	189	0.33
1	100	0.19
2	99	0.19
4	89	0.18

**Table 6.** XPS characterization of KF/ $\gamma$ -Al<sub>2</sub>O<sub>3</sub> catalyst in recycling

Recycling times	K abundance / %	F abundance / %	O abundance / %	Al abundance / %
Fresh catalyst	5.03	5.87	64.94	24.16
1	4.91	5.89	64.49	24.71
4	4.19	6.28	64.89	24.64

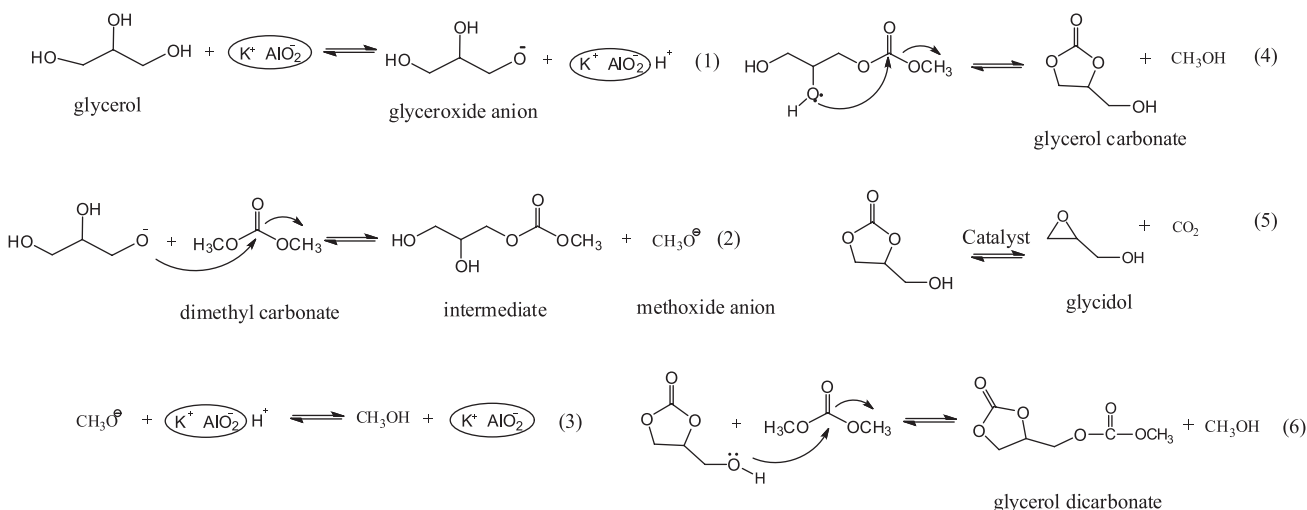


**Figure 5.** Possible reaction mechanism for transesterification of glycerol with DMC.

methanol stayed in the reaction solution would dissolve KOH and partial  $\text{KAlO}_2$  on the catalyst surface gradually. The violent stirring during reaction would further enhance the dissolution rate and lead to the accelerated deactivation of the reused catalyst. Thus, the potassium leaching should be the main reason for the catalyst deactivation.

As mentioned above, the thermal treatment temperature for  $\text{KF}/\gamma\text{-Al}_2\text{O}_3$  affected GC formation slightly at the temperature 100–400 °C, because the formed new basic sites, KOH and  $\text{KAlO}_2$  compensated the loss of coordinately unsaturated  $\text{F}^-$  ion at higher temperatures. However,  $\text{KF}/\gamma\text{-Al}_2\text{O}_3$  dried at 100 °C exhibited lower stability than that calcined at 400 °C. For the first recycling of 15 wt.%  $\text{KF}/\gamma\text{-Al}_2\text{O}_3$  treated at 100 °C, the glycerol conversion decreased from 96.2% to 60.8% over fresh catalyst, indicating that the active coordinately unsaturated  $\text{F}^-$  ion was not stable. In contrast,  $\text{KF}/\gamma\text{-Al}_2\text{O}_3$  calcined at 400 °C showed much higher stability. Glycerol conversion of 90.6% and 85.9% of GC yield were obtained at the fourth recycling. This should be attributed to the formation of new stable  $\text{KAlO}_2$  phases.

#### Proposed mechanism for transesterification of glycerol and DMC

Ochoa-Gómez *et al.*<sup>16</sup> had suggested that basic catalyst with enough basic strength could activate the primary hydroxyl group of glycerol and proposed a reasonable reaction mechanism accordingly. As the reaction by-products, glycidol and glycerol dicarbonate were detected in the mixed products. Gade<sup>41</sup> and Rokicki<sup>7</sup> disclosed the formation of glycidol and glycerol dicarbonate in their research work, respectively. However, few research efforts concerned about the effect of formed methanol

and glycidol. We found that glycerol and DMC could be formed in the reaction of GC and methanol, indicating that the reaction of glycerol with DMC was reversible. Thus, it was advised to remove the formed methanol in order to improve the glycerol conversion.

As to the formation of glycidol, there existed two possible routes. The one resulted from the decomposition of GC, the other was from the direct dehydration of glycerol. For that, the mixture of glycerol and catalyst was heated to 80 °C and kept for 1.5 h. GC, glycidol, glycerol dicarbonate were not detected in the product, indicating that the formation of glycidol was from the decomposition of GC rather than the direct dehydration of glycerol. Furthermore, the interaction<sup>42</sup> of epoxy group with carbon dioxide could confirm that formation of glycidol from GC was also a reversible reaction.

Based on the properties of basic catalyst and product distribution, we proposed a possible mechanism (shown in Figure 5) for the transesterification of glycerol and DMC. The first four steps of possible reaction mechanism illustrated in Figure 5 were similar to the one in reference.<sup>16</sup> However, GC could react reversibly with methanol and produce glycerol. Furthermore, as the side reactions, GC could not only be decomposed to glycidol and  $\text{CO}_2$ , but also react with the excessive DMC to glycerol dicarbonate.

## Conclusions

In summary,  $\text{KF}/\gamma\text{-Al}_2\text{O}_3$  prepared by a wet impregnation way is an efficient solid base catalyst for the synthesis of GC from glycerol and DMC. It was proved that  $[\text{Al}-\text{OH}\cdots\text{F}^-]$ , KOH and  $\text{KAlO}_2$  were the main active basic sites for GC formation. Furthermore, it was obtained that the strong basic sites not only promoted the conversion of glycerol,

but also enhanced the decomposition of GC into glycidol. The deactivation of the catalyst was mainly caused by the leaching of active potassium species. Moreover, elevating the calcination temperature of KF/ $\gamma$ -Al<sub>2</sub>O<sub>3</sub> could retard the deactivation rate. Based on the product distribution, a possible catalytic reaction mechanism was proposed.

## Acknowledgments

We thank the National Key Basic Research and Development Program of China for financial support (Project No. 2012CB215305).

## References

1. Zhou, C. H.; Beltramini, J. N.; Fan, Y. X.; Lu, G. Q.; *Chem. Soc. Rev.* **2008**, *37*, 527.
2. da Silva, G. P.; Mack, M.; Contiero, J.; *Biotechnol. Adv.* **2009**, *27*, 30.
3. Dasari, M. A.; Kiatsimkul, P. -P.; Sutterlin, W. R.; Suppes, G. J.; *Appl. Catal. A: Gen.* **2005**, *281*, 225.
4. Pagliaro, M.; Ciriminna, R.; Kimura, H.; Rossi, M.; Della Pina, C.; *Angew. Chem., Int. Ed.* **2007**, *46*, 4434.
5. Sonnati, M. O.; Amigoni, S.; de Givenchy, E. P. T.; Darmanin, T.; Choulet, O.; Guittard, F.; *Green Chem.* **2013**, *15*, 283.
6. Ubaghs, L.; Fricke, N.; Keul, H.; Höcker, H.; *Macromol. Rapid Commun.* **2004**, *25*, 517.
7. Rokicki, G.; Rakoczy, P.; Parzuchowski, P.; Sobiecki, M.; *Green Chem.* **2005**, *7*, 529.
8. Mei, H.; Zhong, Z.; Long, F.; Zhuo, R.; *Macromol. Rapid Commun.* **2006**, *27*, 1894.
9. Burk, R. M.; Roof, M. B.; *Tetrahedron Lett.* **1993**, *34*, 395.
10. Mizuno, T.; Nakai, T.; Mihara, M.; *Heteroat. Chem.* **2010**, *21*, 99.
11. Hu, J.; Li, J.; Gu, Y.; Guan, Z.; Mo, W.; Ni, Y.; Li, T.; Li, G.; *Appl. Catal. A: Gen.* **2010**, *386*, 188.
12. Vieville, C.; Yoo, J.; Pelet, S.; Mouloungui, Z.; *Catal. Lett.* **1998**, *56*, 245.
13. George, J.; Patel, Y.; Pillai, S. M.; Munshi, P.; *J. Mol. Catal. A: Chem.* **2009**, *304*, 1.
14. Climent, M. J.; Corma, A.; De Frutos, P.; Iborra, S.; Noy, M.; Velty, A.; Concepción, P.; *J. Catal.* **2010**, *269*, 140.
15. Hammond, C.; Lopez-Sanchez, J. A.; Ab Rahim, M. H.; Dimitratos, N.; Jenkins, R. L.; Carley, A. F.; He, Q.; Kiely, C. J.; Knight, D. W.; Hutchings, G. J.; *Dalton Trans.* **2011**, *40*, 3927.
16. Ochoa-Gómez, J. R.; Gómez-Jiménez-Aberasturi, O.; Maestro-Madurga, B.; Pesquera-Rodríguez, A.; Ramírez-López, C.; Lorenzo-Ibarreta, L.; Torrecilla-Soria, J.; Villarán-Velasco, M. C.; *Appl. Catal. A: Gen.* **2009**, *366*, 315.
17. Bell, J. B.; *US Pat.* **2,915,529** **1959**.
18. Alvarez, M. G.; Segarra, A. M.; Contreras, S.; Sueiras, J. E.; Medina, F.; Figueras, F.; *Chem. Eng. J.* **2010**, *161*, 340.
19. Bai, R.; Wang, Y.; Wang, S.; Mei, F.; Li, T.; Li, G.; *Fuel Process. Technol.* **2013**, *106*, 209.
20. Kim, S. C.; Kim, Y. H.; Lee, H.; Yoon, D. Y.; Song, B. K.; *J. Mol. Catal. B: Enzym.* **2007**, *49*, 75.
21. Grey, R. A.; *US Pat.* **5,091,543** **1992**.
22. Naik, P. U.; Petitjean, L.; Refes, K.; Picquet, M.; Plasseraud, L.; *Adv. Synth. Catal.* **2009**, *351*, 1753.
23. Takagaki, A.; Iwatani, K.; Nishimura, S.; Ebitani, K.; *Green Chem.* **2010**, *12*, 578.
24. Clark, J. H.; *Chem. Rev.* **1980**, *80*, 429.
25. Ando, T.; Brown, S. J.; Clark, J. H.; Cork, D. G.; Hanafusa, T.; Ichihara, J.; Miller, J. M.; Robertson, M. S.; *J. Chem. Soc., Perkin Trans. 2* **1986**, 1133.
26. Wen, L.; Ji, C.; Li, Y.; Li, M.; *J. Comb. Chem.* **2009**, *11*, 799.
27. Qiu, P.; Yang, B.; Yi, C.; Qi, S.; *Catal. Lett.* **2010**, *137*, 232.
28. Ando, T.; Clark, J. H.; Cork, D. G.; Hanafusa, T.; Ichihara, J.; Kimura, T.; *Tetrahedron Lett.* **1987**, *28*, 1421.
29. Vazquez, A.; Lopez, T.; Gomez, R.; Morales, A.; Novaro, O.; *J. Solid State Chem.* **1997**, *128*, 161.
30. Xie, W.; Peng, H.; Chen, L.; *Appl. Catal. A: Gen.* **2006**, *300*, 67.
31. Hoydonckx, H. E.; De Vos, D. E.; Chavan, S. A.; Jacobs, P. A.; *Top. Catal.* **2004**, *27*, 83.
32. Gerpen, J. V.; *Fuel Process. Technol.* **2005**, *86*, 1097.
33. Tanabe, K. In *Catalysis by Acids and Bases*; Tanabe, K.; Imelik, B., eds.; Elsevier: Amsterdam, 1985.
34. Wan, T.; Yu, P.; Gong, S.; Li, Q.; Luo, Y.; *Korean J. Chem. Eng.* **2008**, *25*, 998.
35. Murugan, C.; Bajaj, H.; *Fuel Process. Technol.* **2011**, *92*, 77.
36. Zhu, J. H.; Xu, Q. H.; *Acta Chim. Sinica* **1997**, *55*, 474.
37. Verziu, M.; Florea, M.; Simon, S.; Simon, V.; Filip, P.; Parvulescu, V. I.; Hardacre, C.; *J. Catal.* **2009**, *263*, 56.
38. Alonso, D. M.; Mariscal, R.; Moreno-Tost, R.; Poves, M.; Granados, M. L.; *Catal. Commun.* **2007**, *8*, 2074.
39. Castro, C. S.; Cardoso, D.; Nascente, P. A.; Assaf, J. M.; *Catal. Lett.* **2011**, *141*, 1316.
40. Di Serio, M.; Mallardo, S.; Carotenuto, G.; Tesser, R.; Santacesaria, E.; *Catal. Today* **2012**, *195*, 54.
41. Gade, S. M.; Munshi, M. K.; Chherawalla, B. M.; Rane, V. H.; Kelkar, A. A.; *Catal. Commun.* **2012**, *27*, 184.
42. Li, Z.; Zhao, Y.; Yan, S.; Wang, X.; Kang, M.; Wang, J.; Xiang, H.; *Catal. Lett.* **2008**, *123*, 246.

Submitted: August 2, 2013

Published online: November 29, 2013